# Experimental Studies of Unsteady Trailing-Edge Conditions

Bodapati Satyanarayana* and Sanford Davis†
*NASA Ames Research Center, Moffett Field, Calif.*

**In the prediction of unsteady pressure distributions over airfoils, the steady-state Kutta-Joukowsky condition usually is assumed. Recent experimental investigations show that the pressure differential at the trailing edge approaches zero at lower reduced frequencies ($k<0.1$), whereas substantial deviations are reported at higher reduced frequencies ($k>5$). This paper describes an investigation to find the range of reduced frequencies over which the classical Kutta-Joukowsky condition is valid and the nature of deviations beyond this range. An NACA 64A010 airfoil with a 15-cm chord is supported between the side walls of a 25- ×35-cm low-speed wind tunnel and oscillated over reduced frequencies ranging from 0.05 to 1.2. The experimentally determined loading near the trailing edge is measured and compared with unsteady, incompressible, small-disturbance theory. Experimental data are obtained both with and without a boundary-layer trip. It is observed that application of the Kutta-Joukowsky condition in the theoretical analysis is valid below a reduced frequency of about 0.6 in predicting the loading in the trailing-edge region. At reduced frequencies beyond 0.8, the predicted results underestimate the measured loading near the trailing edge, and the deviations increase further with reduced frequency. Similarly, the experimental phase angle of the loading in the trailing-edge region agrees reasonably with the linear theory up to $k=0.8$ but lags the predicted value beyond $k=0.8$.**

## Nomenclature

| | |
|---|---|
| $C$ | = airfoil chord |
| $C_p$ | = unsteady pressure coefficient = unsteady pressure/$(\frac{1}{2}\rho U_\infty^2)$ |
| $f$ | = frequency of oscillation, Hz |
| $k$ | = reduced frequency = $\omega C/2U_\infty$ |
| mag( ) | = magnitude of complex quantity mag$(a+ib)$ $=\sqrt{a^2+b^2}$ |
| ph( ) | = phase of complex quantity ph$(a+ib)=\tan^{-1}(b/a)$ |
| $U_\infty$ | = freestream velocity |
| $X$ | = distance from leading edge |
| $\alpha$ | = angle of attack, deg |
| $\omega$ | = angular frequency $(=2\pi f)$, rad/s |
| $\rho$ | = density |
| $\Delta C_p$ | = unsteady pressure loading = $C_{p_{\text{lower}}} - C_{p_{\text{upper}}}$ |
| $\Delta C_{p,\alpha}$ | = unsteady pressure loading per degree |

## Introduction

IN predicting the steady and unsteady inviscid pressure distribution over an airfoil, the steady-state Kutta-Joukowsky condition normally is applied. This empirical viscous criterion avoids an infinite velocity in the flow around a sharp point by postulating that the rear stagnation point be fixed at the trailing edge. For rounded trailing edges, the position of the rear stagnation point is indeterminate, and the circulation must be determined by the effect of viscosity on the trailing-edge flow. Gostelow[1] discusses the applicability of the Kutta-Joukowsky condition for various trailing-edge geometries in steady and unsteady flows.

In the unsteady case, the problem is complicated further by the unsteady boundary layer and wake. The usual assumption of no unsteady loading at the trailing edge has been applied in the theoretical analysis of airfoils and cascades. This condition is now being questioned, particularly at high reduced frequencies. Even if deviations in the loading in the trailing-edge region do not affect the unsteady lift, the contribution to the moment is considerable. The deviations in phase are especially important. Therefore, the correct theoretical modeling of the generalized trailing-edge condition is important in evaluating the unsteady lift and moment under various conditions. Sears[2] recently proposed that the lift, moment, and vortex strength distributions can be obtained from a vortex-sheet model as in the classical thin-airfoil theory, but the circulation for this model has to be determined from a second model, which includes boundary-layer effects. McCroskey[3] has reviewed the subject briefly.

It has been observed experimentally[4] that the gust-induced pressure differential at the trailing edge of the nonlifting symmetrical airfoil (10C4 section), both isolated and in a cascade, approaches zero at low reduced frequencies ($k<0.1$), although deviations from theory were reported in phase angle. These experiments were conducted in a specially built gust tunnel. Recently, Osdiek[5] measured the pressure distribution on an airfoil in a cascade at low reduced frequency ($k=0.08$), and his results deviated from the predicted results in the trailing-edge region, although the agreement is very good in the leading-edge region. The unsteady flow in this case is created by the oscillation of an inlet section, and the mean angle of attack is varied between 6 and 12 deg.

Archibald[6] measured the pressure differential near the trailing edge of a flat plate and an airfoil at high reduced frequencies ($k>5.0$) and showed that the Kutta condition does not hold. In this case, the unsteady flow in the test section was created by exciting two loudspeakers connected in antiphase. Fujita and Kovasznay[7] reported on the response of a stationary instrumented airfoil to the wake of an upstream rotating rod. The measured chordwise response was in good agreement with linear theory over most of the chord except for the last 10%. In this region, theoretical agreement was poor because of loading at the trailing edge. But Commerford and Carta[8] concluded from experiments on a circular arc airfoil that "the individual pressure distributions at each angle of attack tend to zero at the trailing edge indicating that the Kutta condition was satisfied even at this high reduced frequency." However, the agreement with phase was very poor. The periodically fluctuating flowfield was produced by the natural shedding of vortices from a transverse cylinder to

Received March 14, 1977; presented as Paper 77-450 at the AIAA Dynamics Specialist Conference, San Diego, Calif., March 24-25, 1977; revision received Sept. 23, 1977. 

Index categories: Nonsteady Aerodynamics, Subsonic Flow; Transonic Flow.

*NRC Research Associate; presently Engineering Senior Research Associate, Joint Institute for Aeronautics and Acoustics, Department of Aeronautics and Astronautics, Stanford University, Stanford, Calif. Member AIAA.

†Research Scientist. Member AIAA.

yield a reduced frequency of 3.9. In this case, the last chordwise measurement was taken at 90% chord, and the agreement was particularly good. However, the agreement with theory in the leading-edge region was not so good, indicating that the agreement at 90% chord was probably fortuitous.

Another example of the failure of the Kutta condition at high reduced frequency ($k \approx 5$) was reported by Davis[9] in connection with measurements of aerodynamic noise. Aerodynamic measurements of the noise generated by a modified NACA 64A006 airfoil section show the free-field directivity pattern to be cardioid-shaped and centered at the trailing edge as predicted by him[10] for the case when no Kutta condition is applied at the trailing edge.

Since the acoustic directivity pattern is so sensitive to the trailing-edge conditions, it is important to determine the frequency range over which the classical Kutta-Joukowsky condition holds. The reader is referred to the papers by Orszag and Crow[11] and Bechert and Pfizenmaier[12,13] on the unsteady condition as applied at the lip of a nozzle. Yates[14] calculated the pressure distribution on the trailing edge of a semi-infinite airfoil oscillating in a subsonic parallel shear flow and discussed the results obtained with and without a Kutta conditon.

Because of the importance of these effects to unsteady aerodynamics, it is of interest to find the range of reduced frequency over which the classical Kutta-Joukowsky condition is valid and the nature of the deviations beyond this range so that prediction methods can be modified accordingly. This paper describes an investigation to clarify this problem.

## Experimental Apparatus

The experiments were conducted in a 25-cm-wide × 35-cm-high × 100-cm-long indraft-type wind tunnel. Steady uniform flow was obtained by choking the flow downstream of the test section. Although the flow speed could be varied by interchanging nozzle blocks downstream of the test section, all of the results presented in this paper were obtained at a nominal speed of 58 m/s (190 ft/s). Low turbulence (turbulence intensity < 0.1%) was obtained with six screens in the 75-cm-long contraction.

A NACA 64A010 airfoil fabricated of compressed wood with a 15-cm chord and 25-cm span was instrumented with four 2.4-mm-diam × 9.5-mm-long unsteady pressure transducers. Pressure orifices were provided at 40% chord and in the trailing-edge region on both upper and lower surfaces at 89.3%, 92%, 94%, and 97.3% chord. The pressure was measured using the two transducers located at 85% chord connected to one hole on each surface at a time and blocking the other pressure taps with mylar type. Simultaneous measurements also were made at the 40% chord position. Static pressure taps also were provided at the same chordwise locations. The tests were conducted with and without a boundary-layer trip consisting of randomly distributed 0.38-mm glass balls over a width of 3.2 mm starting 9.5 mm from the leading edge. The transducer leads and static pressure tubes were taken out through a 6-mm-o.d. hollow rod at the 25% chord position. The transducers in the trailing-edge region were embedded in the airfoil at the aftmost physically possible location of 85% chord. A schematic diagram of the test section with oscillating airfoil model is shown in Fig. 1 and a schematic of the instrumented airfoil in Fig. 2.

The airfoil was oscillated about an axis at 25% chord with a 25-lb electrodynamic shaker. The shaker was connected to the rod by a 5.5-cm-long lever arm. The shaker was driven by a sine-wave signal generator and power amplifier. The signal generator also provided a once-per-cycle reference pulse for data initiation. Schlieren photographs of the wake of the oscillating airfoil show a well-defined thin vortex sheet which implies that the flow is probably well approximated by two-dimensional theory.

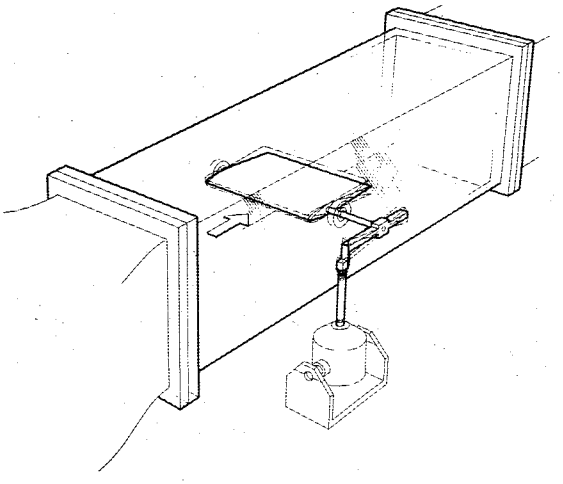

**Fig. 1 Schematic diagram of the 25- × 35-cm wind-tunnel test section with oscillating airfoil model.**

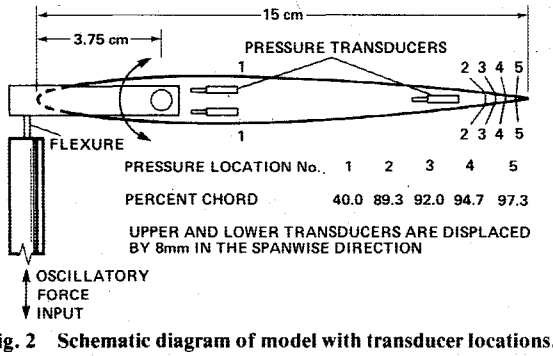


**Fig. 2 Schematic diagram of model with transducer locations.**

## Data Acquisition

The unsteady data were acquired on-line with a Data General Eclipse model S/200 minicomputer. The unsteady signal from the pressure transducer was filtered, amplified, and transported through a 50-m cable to the computer room. The raw data signals at the computer input were contaminated from a variety of sources. However, the signal-to-noise ratio was considerably improved by utilizing the technique of "signal averaging" or "phase-lock averaging." A reference pulse from the signal generator which oscillated the wing was used to initiate the data acquisition process. The data were acquired in short bursts, where each burst was initiated at exactly the same phase position. Each three-to-four-cycle burst then was summed to the previous one. In this manner, all data that are incoherent with the oscillatory motion average to zero, and only the desired coherent signal is retained. A block diagram of the unsteady data acquisition system is shown in Fig. 3.

The data sampling rate was adjusted at each frequency to obtain a 60-point/cycle record (resolution of 6 deg between data points). The number of averaging operations needed was determined on-line by comparing the raw signal and the averaged signal on the CRT display. It was found that good signals could be obtained with 100 averaging operations. In all, seven channels of unsteady data were obtained: four unsteady pressures, the shaker signal, the instantaneous alpha signal (resolver), and a reference accelerometer signal.

Mean static pressures on the airfoil and tunnel reference conditions also were recorded on-line with a scanning-valve-type pressure transducer. The mean model incidence was set to zero by observing the mean static pressures on the upper and lower surfaces at 40% chord. The steady and unsteady pressure transducers were calibrated frequently during the test.

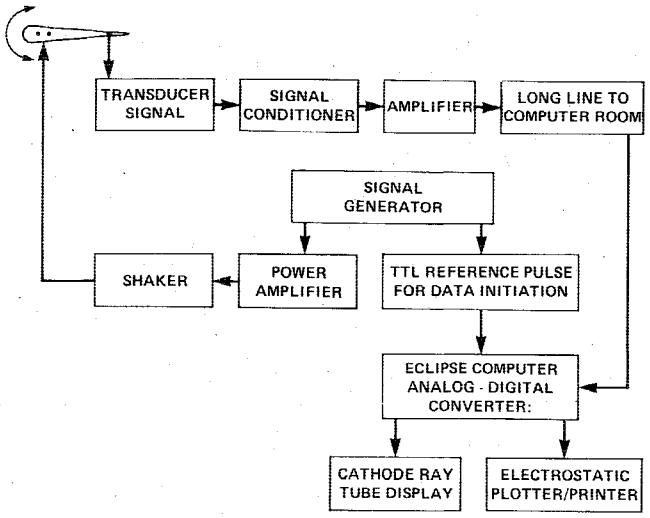


**Fig. 3 Block diagram for unsteady data acquisition.**

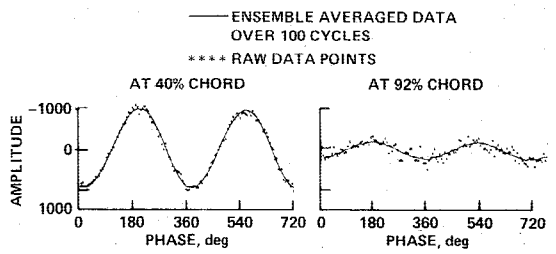


**Fig. 4 Typical raw data and ensemble-averaged data pressure traces at 40% and 92.0% chord.**

All of the experiments reported in this paper were conducted at a nominal freestream velocity of 59 m/s ($M=0.168$) and a chord Reynolds number of 560,000. The freestream velocity was corrected for blockage. The airfoil was oscillated at frequencies ranging from 6 to 150 Hz, which corresponds to a reduced frequency ($k$) range of 0.05 to 1.2 based on half-chord. The airfoil was oscillated up to approximately ±1-deg incidence at a mean angle of attack of 0 deg. The incidence range available was low at higher frequencies. The experiments were conducted both with and without transition boundary-layer trip. During each correlation, the mean and unsteady pressures, the wind-tunnel test conditions, and the ambient conditions were recorded on-line with the minicomputer.

## Data Reduction and Presentation of Results

The experimental unsteady pressure coefficients were obtained by multiplying the transducer signals by the appropriate transducer constants and dividing by dynamic pressure. Previous calibrations have shown that Kulite pressure transducers have frequency response characteristics that are flat from dc to 40 kHz, and so static calibrations were applied in analyzing the results. Although the alpha signal (resolver) was linear with incidence for the static calibration, it was observed that the calibration constant was frequency dependent. Although later on the resolver was calibrated dynamically at all tested frequencies, the following procedure was used to determine the equivalent angle of attack (complex amplitude). First the unsteady loading was obtained using incompressible, small-disturbance theory. The experimental unsteady loading at 40% chord was matched in magnitude and phase to the predicted value at 40% chord, and the equivalent complex amplitude of the angle of attack was evaluated. This equivalent incidence, which corresponds approximately to the dynamically calibrated incidence, was used in all further calculations. The phase of this equivalent incidence subsequently was compared to accelerometer data. For those frequencies where the accelerometers were moving in phase with the airfoil, the computed incidence based on accelerometer data was within 6 deg of the equivalent incidence.

Typical raw data and data averaged over 100 cycles are presented in Fig. 4 at 40% and 92% chord. The raw data near the trailing edge are noisy compared with the 40% chord data because of the effect of viscosity. Even with a high noise-to-signal ratio, a coherent pressure signal can be extracted and analyzed using signal-averaging techniques.

The signal-averaged data were Fourier analyzed up to the fifth harmonic. In most cases, the signal is dominated by the fundamental frequency. In order to determine the complex amplitude of the equivalent angle of attack, the complex amplitude of only the first harmonic was matched to the predicted loading based on linear, small-disturbance theory.

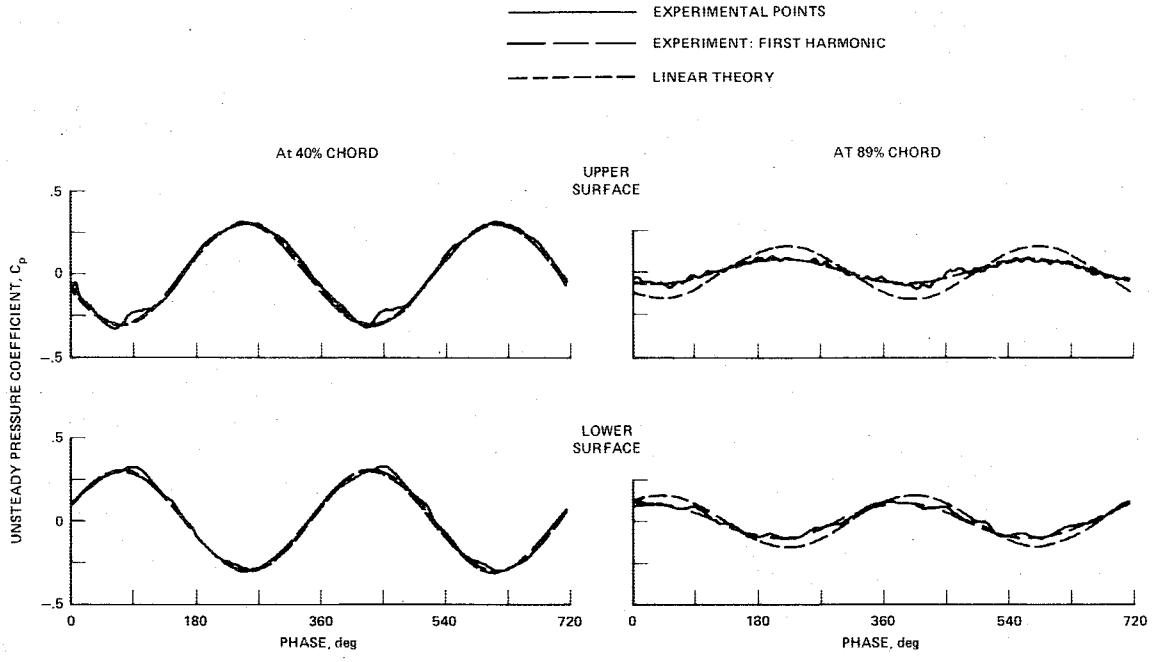


**Fig. 5 Comparison of experimental unsteady pressure distribution with first-harmonic fit and linear theory ($k=0.49$).**

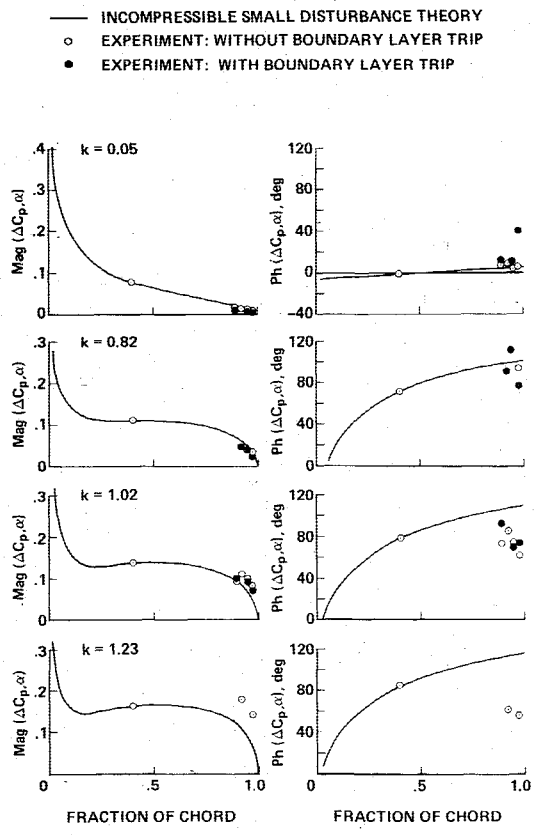


**Fig. 6 Comparision of experimental chordwise unsteady pressure and phase distribution with predicted results at various reduced frequencies.**

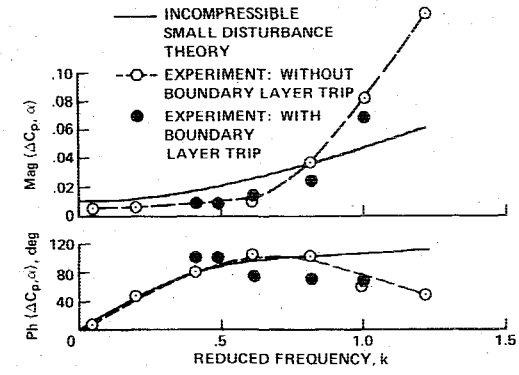


**Fig. 7 Variation of unsteady loading with reduced frequency at 97.3% chord.**

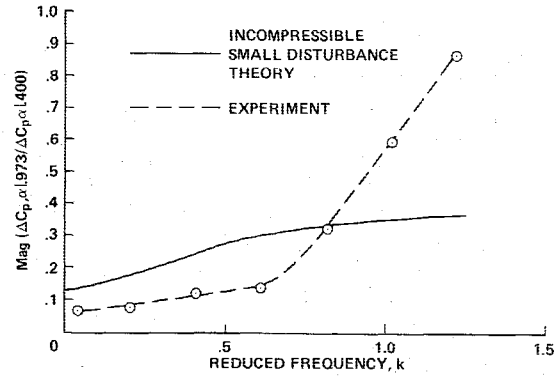


**Fig. 8 Variation of the ratio of trailing-edge loading to 40% chord loading, with reduced frequency.**

Typical upper and lower surface pressure traces at 40% and 89.3% chord are presented in Fig. 5 for $k=0.49$. It can be observed that the first harmonic dominates, and comparisons between theory and experiment based on the first harmonic only are valid. At 40% chord, the upper and lower surface magnitudes are equal but are out of phase by 180 deg, as predicted by theory.

The exact agreement with theory and experiment at 40% chord was due to the manner in which the complex amplitude of the equivalent alpha signal was calculated. In the trailing-edge region, the agreement is fair, with experimental amplitudes about half of the theoretical prediction. This disagreement is not due to the failure of the Kutta-Joukowsky condition but to boundary-layer displacement effects near the trailing edge.[15] Viscosity is also the cause of the jagged appearance of the experimental data.

The magnitude and phase of the predicted and measured first harmonic of the complex amplitude of the loading per unit angle are presented in Fig. 6 for four reduced frequencies. Experimental results with and without boundary-layer transition trip are shown. As discussed previously, the predicted results were matched exactly at 40% chord. At the low reduced frequency of $k=0.05$, the magnitude of $\Delta C_{p,\alpha}$ in the trailing-edge region is less than the predicted value. This trend at low reduced frequencies is attributed to the viscous effects as discussed by Tijdeman.[15] The phase agrees reasonably well at this frequency. As the reduced frequency increases to 0.8, the experimentally determined phase deviates from the predicted value, but the magnitude agrees reasonably well. At a reduced frequency of 1.02, the deviation in both magnitude and phase increases, and, at $k=1.23$, the failure of the classical Kutta-Joukowsky condition in the linear theory is obvious. Although there is some scatter in the phase distribution, there is a very definite increase in aft loading magnitude and a decrease in phase at high frequencies.

## Discussion of Results

The salient results of the investigation are presented in Fig. 7 with magnitude and phase of the complex amplitude at $X/C=0.973$ as ordinates, and reduced frequency $k$ as abscissa. The experimental results with and without a boundary-layer transition trip are compared with linear, incompressible, small-disturbance theory. Thickness and viscous effects are not included in the linear theory, and the usual steady-state Kutta-Joukowsky condition is assumed. It is believed that thickness effects are not important for the range of parameters investigated in this experiment. However, by neglecting viscous effects, linear theory predicts higher loading than was measured at low reduced frequencies. As the reduced frequency increases, the decreased loading due to boundary-layer displacement effects is overwhelmed by the evident failure of the Kutta condition. The magnitude of the unsteady loading increases well beyond that predicted by linear theory, and the phase drops below the theoretical predictions. Between $k=0.6$ and 0.8, there is a marked difference in the rate of increase of the loading with reduced frequency. The experimental phase agrees reasonably well with the predicted values up to $k=0.8$ but lags the predicted value for all conditions beyond $k=0.8$, the deviation increasing with frequency. Experimental results with a boundary-layer trip also are presented in the same figure. Although there is some discrepancy in the phase values, there is no marked difference in the result. The similar trends with and without the trip indicate that there are no important Reynolds number effects at these low oscillation amplitudes.

The variation of the ratio of loading at 97.3% chord to 40% chord with reduced frequency is presented in Fig. 8 and also compared with linear theory. The trends are similar to the results in Fig. 7.

The averaged pressure traces at 40% and 97.3% chord are presented in Fig. 9 for two different oscillation amplitudes at $k=0.2$. At the higher amplitude, the suction peak is cut off. If

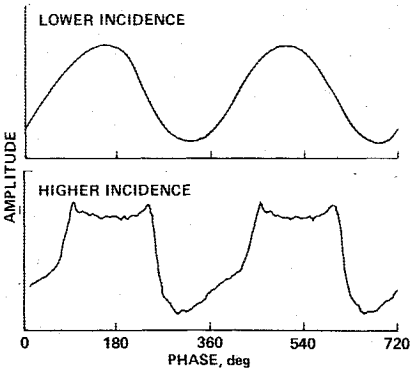


**Fig. 9 Effect of amplitude on unsteady pressure distribution in the trailing-edge region.**

the amplitude is increased further, the flat portion becomes concave, effectively doubling the frequency. This effect at higher amplitudes is due to instantaneous separation. In the absence of separation, the frequency of the pressure signal should have the same frequency as the airfoil motion. These effects are similar to the results presented in Ref. 16, where it is shown that, when the flow separates on one surface, the pressure on both surfaces tends to equalize, effectively doubling the frequency.

## Conclusions

1) Application of the Kutta-Joukowsky condition is valid below a reduced frequency of 0.6 in predicting the pressure differential in the trailing-edge region. For reduced frequency beyond 0.8, application of the Kutta-Joukowsky condition predicts lower pressure differentials in the trailing-edge region. The deviations increase with reduced frequencies in the range of 0.8 to 1.2.

2) The experimental phase angles in the trailing-edge region reasonably agree with the predicted values up to $k = 0.8$ but lag the predicted value beyond 0.8.

3) For low oscillation amplitudes, the experimental pressure traces can be approximated by the first harmonic wihout suffering in accuracy.

4) At higher amplitudes of oscillation (much lower than the stall angle), the pressure trace in the trailing-edge region exhibits frequency doubling.

## References

[1] Gostelow, J. P., "Trailing Edge Flows Over Turbomachine Blades and the Kutta-Joukowsky Condition," American Society of Mechanical Engineers, Paper 75-GT-9A, March 1975.

[2] Sears, W. R., "Unsteady Motion of Airfoils with Boundary Layer Separation," *AIAA Journal*, Vol. 14, Feb. 1976, pp. 216-220.

[3] McCroskey, W. J., "Some Current Research in Unsteady Fluid Dynamics," *Journal of Fluids Engineering*, Vol. 99, March 1977.

[4] Satyanarayana, B., "Unsteady Wake Measurements of Airfoils and Cascades," AIAA Paper 76-7, Washington, D.C., 1976; also *AIAA Journal*, Vol. 15, May 1977, pp. 613-618.

[5] Osdiek, F. R., "A Cascade in Unsteady Flow," AGARD CP 177, 1975.

[6] Archibald, F. S., "Unsteady Kutta Condition at High Values of the Reduced Frequency Parameter," *Journal of Aircraft*, Vol. 12, June 1975, pp. 545-550.

[7] Fujita, H. and Kovasznay, L. S. G., "Unsteady Response of an Airfoil to Wake Cutting," *AIAA Journal*, Vol. 12, Sept. 1974, pp. 1216-1221.

[8] Commerford, G. L. and Carta, F. O., "Unsteady Aerodynamic Response of a Two-Dimensional Airfoil at High Reduced Frequency," *AIAA Journal*, Vol. 12, Jan. 1974, pp. 43-48.

[9] Davis, S. S., "Measurements of Discrete Vortex Noise in a Closed-Throat Wind Tunnel," *AIAA Progress in Astronautics and Aeronautics—Aeroactoustics: STOL Noise; Airframe and Airfoil Noise*, Vol. 45, edited by I. R. Schwartz, 1976, pp. 237-257.

[10] Davis, S. S., "Theory of Discrete Vortex Noise," *AIAA Journal*, Vol. 13, March 1975, pp. 375-380.

[11] Orszag, S. A. and Crow, S. C., "Instability of Vortex Sheet Leaving a Semi-Infinite Plate," *Studies in Applied Mathematics*, Vol. XLIX, June 1970, pp. 167-181.

[12] Bechert, D. and Pfizenmaier, E., "On the Kutta Condition at the Nozzle Discharge Edge in a Weakly Unsteady Nozzle Flow," Royal Aircraft Establishment Library Transl. 1617, D.L.R. Rept. FB 71-09, Sept. 1971 (in German).

[13] Bechert, D. and Pfizenmaier, E., "Optical Compensation Measurements on the Unsteady Exit Condition at a Nozzle Discharge Edge," *Journal of Fluid Mechanics*, Vol. 71, Pt. 1, 1975, pp. 123-144.

[14] Yates, J. E., "Pressure Distribution on the Trailing Edge of a Semi-Infinite Airfoil Oscillating in a Shear Layer," AIAA Paper 77-157, Los Angeles, Calif., 1977.

[15] Tijdeman, H., "On the Unsteady Aerodynamic Characteristics of Oscillating Airfoils in Two-Dimensional Transonic Flow," *Office of Naval Research Transonic Flow Conference*, Los Angeles, Calif., March 1976.

[16] Satyanarayana, B., "Some Aspects of Unsteady Flow Past Airfoils and Cascades," AGARD CP 177, 1975.